Progress In Electromagnetics Research M, Vol. 77, 17–28, 2019

Single-Feed Single-Patch Triple-Band Single-Beam/Dual-Beam U-Slotted Patch Antenna

Huaxiao Lu*, Yuan'an Liu, Fang Liu, and Weimin Wang

Abstract—A novel single probe-fed, single-layer, and single-patch triple-band microstrip antenna is presented. By incorporating two identical U-slots in the patch whose length is λ_d instead of $1/2\lambda_d$ in a conventional patch, three operating bands are achieved. Dual-beam radiation pattern is obtained at the upper band, and a single broadside beam radiation pattern is obtained at each of the lower and middle bands. The antenna's structure is simple. Only by using a single probe-fed point, the impedance matches well at all the three resonant frequencies. The measured and simulated results are in good agreement. The measured lower, middle, and upper bands are centered at 2.442 GHz, 3.505 GHz, and 5.787 GHz, respectively. The measured gains are 6.2 dBi at 2.442 GHz and 5.5 dBi at 3.505 GHz, respectively. At 5.787 GHz, the measured gains for the dual radiation beams are 8.4 dBi directed at 26° and 8.2 dBi directed at −38°, respectively. The proposed antenna can be a candidate for WLAN 2.4 GHz, WLAN 5.8 GHz, and 3.5 GHz of 5G (the fifth-generation mobile communication) operation.

1. INTRODUCTION

The rapid development of modern wireless communication requires multiband antennas. There have been many techniques to design dual-band or triple-band antennas in the published literature. However, for triple-band antennas, most of them are monopole antennas [1–3] or dipole antennas [4, 5]. These antennas generally have wideband characteristics, but their radiation beams are omnidirectional or bidirectional. This reduces the antenna directivity and gain [6], and their back radiations bring interference to circuits which are assembled below the ground plane [7]. Microstrip antenna is a popular candidate in modern wireless communication because it has the advantages of low cost, low profile, lightweight, compactness, and easy integration with other circuits. There are many reports on microstrip antennas with dual-band [8–11] in published literature, and these dual-band antennas are either single layer [8–10] or stacked structure [11]. However, there are not many reports on microstrip antennas with triple-band [12–14] in published literatures. In [12], two pairs of different arc slots and eight stubs are cut in a rectangular patch to realize triple-band characteristic. In [13], a rectangular patch loaded with two different slots and a ground plane loaded with two identical L-shaped slots, two identical asymmetrical U-slots, and two identical rectangular ring-slots are used to realize the triple-band characteristic. Meanwhile, the antenna is fed by a microstrip line. In [14], two different stub-loaded concentric annular-rings and an inside small circular patch are used to realize the triple-band characteristic, and a cross-slot embedded in the ground plane is used to reduce the antenna size, but this cross-slot increases the back radiation. These triple-band antennas maintain the advantage of single layer, but their radiating elements are relatively complicated. Meanwhile, the gains of these antennas are not high enough. For instance, the gains for the triple-band antenna in [12] at the three resonant frequencies are 3.1 dBi, 4.4 dBi, and 2 dBi, respectively. The gains for the triple-band antenna

Received 1 September 2018, Accepted 23 October 2018, Scheduled 13 December 2018
* Corresponding author: Huaxiao Lu (huaxiaous@126.com).
The authors are with the School of Electronic Engineering, Beijing University of Posts and Telecommunications, Beijing 100876, China.

in [13] are 0.32 dBi, 1.2 dBi, and 1.5 dBi, respectively, and that for the triple-band antenna in [14] are 0.5 dBi, −0.5 dBi, and 2.1 dBi, respectively. Compared to aperture coupled feed or stacked structures which need relatively complex feeds or more than one layer or more than one patch, single feed single layer single patch antennas have attracted much attention due to the simple structure.

Dual/multi-beam antennas are antennas which have more than one directional beam from a single aperture, and they have the ability of covering multiple areas, which is useful for wireless communication or radar systems because the number of the required antennas is reduced, and the link quality is improved [15]. A wideband E-shaped patch antenna with dual-beam across the operating bandwidth is reported in [16]. A wideband dual-beam patch antenna with a cross-shaped probe is reported in [17]. To the best of the authors' knowledge, in the published literature for realizing triple-band antennas, there is no published report on at least one band operating with dual radiation beams.

In this work, a triple-band microstrip antenna with two U-slots is presented and investigated. The antenna has only one feed, only one layer, and only one rectangular patch with two identical U-slots. The proposed antenna exhibits a single beam at the lower and middle bands, respectively, and exhibits a dual-beam at the upper band. The proposed antenna has the following advantages: (1) Its structure is simple, simpler than many other antennas designed for realizing triple-band characteristic. (2) One of the three bands, that is the upper band, is operating with dual-beam. (3) The feed is simple, and only by a single probe feed point, the proposed antenna matches well at all the three resonant frequencies. The current distributions on the surface of the U-slots loaded patch are presented to analyze the proposed antenna. Parametric studies on several parameters are presented. Furthermore, the parametric study on the arm length of the U-slots is carried out to demonstrate that the three resonant frequencies can be adjusted by tuning the arm length, which is more convenient than that reported in [18], where the two resonant frequencies can be adjusted through the shorting walls. The proposed antenna can switch from a triple-band one to a dual-band one by tuning the arm length of the U-slots as well. The measured and simulated results are in good agreement, and satisfactorily low cross-polarization levels are achieved due to the symmetric structure. The radiating element volume of the proposed antenna is $0.37\lambda_g \times 0.16\lambda_g \times 0.02\lambda_g$ (λ_g is the wavelength in the substrate at the lower resonant frequency), which is much smaller than that in [9, 10, 12]; meanwhile, the antenna's gain is high enough. The design guidelines in this work provide guidance for the antenna's design in theory, which is useful to reduce the cost time for design optimization.

2. ANTENNA CONFIGURATION AND DESIGN

2.1. Antenna Geometry

The configuration of the proposed antenna is shown in Fig. 1. The rectangular patch's length L_R is λ_d instead of $\lambda_d/2$ in a conventional microstrip antenna (λ_d is the wavelength in the substrate). For the sake of easy fabrication with printing technology, this rectangular patch is printed over a Rogers 4350 dielectric substrate with thin thickness of 0.762 mm, relative permittivity of 3.48, and loss tangent $\tan\sigma = 0.004$. Two identical U-slots were symmetrically cut close to both the radiating edges and the nonradiating edges of the rectangular patch, respectively. Air, with thickness $h = 3$ mm and relative permittivity $\varepsilon_r = 1$, is used as the substrate. The patch is supported on the ground plane by plastic bolts. The dimension of the ground plane is $L_G \times W_G = 68\,\text{mm} \times 43\,\text{mm}$. The overall antenna is geometrically symmetric along either the x-axis or the y-axis, which can maintain a low cross-polarization. An SMA connecter is used to feed the antenna, and the diameter of the coaxial probe is 1.3 mm. The final dimensions of the proposed antenna are given in Table 1.

Table 1. The dimensions of the proposed antenna.

Parameters	L_R	W_R	d_V	d_H	U_C	U_L	d_P
Values (mm)	45	20	1	1	1	8	4.5

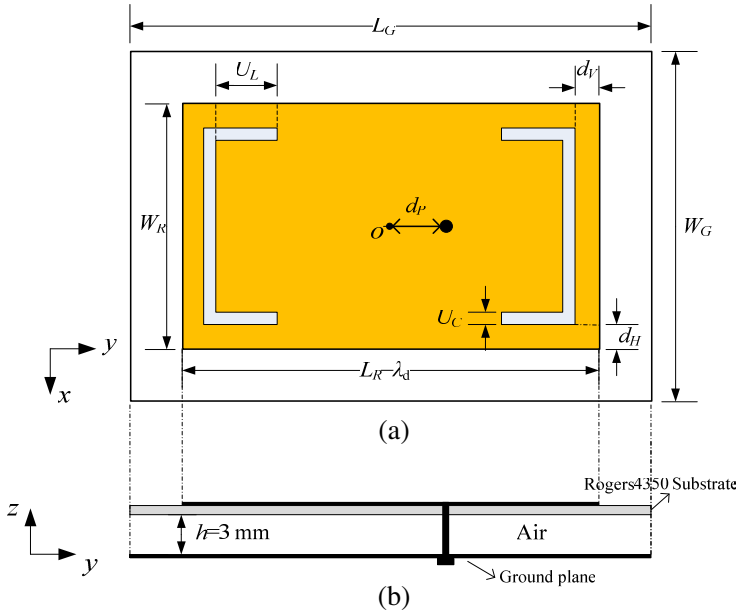

Figure 1. The configuration of the proposed antenna: (a) top view; (b) side view.

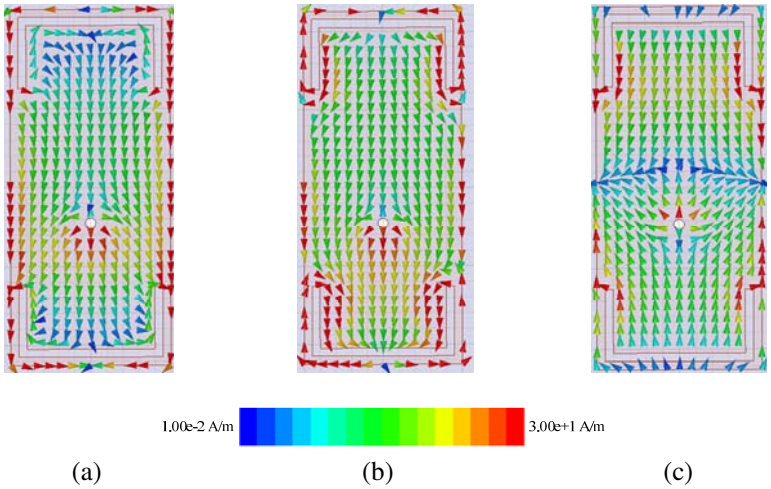

Figure 2. The simulated current distributions at: (a) f_L (2.444 GHz); (b) f_M (3.509 GHz); (c) f_U (5.823 GHz).

2.2. Antenna Analysis and Design Guidance

A conventional patch antenna with its length of $\lambda_d/2$, has a single beam radiation pattern. For the proposed antenna, its surface current distributions at the three resonant frequencies, the lower, middle, and upper resonant frequencies, denoted as f_L, f_M, and f_U (each of them is defined as the minimum value of S_{11} in its corresponding operating band), respectively, are presented in Fig. 2. Based on the cavity model of the patch antenna [19], the two maxima on the surface current of the rectangular patch, as shown in Fig. 2(c), suggest that the upper resonant frequency operates at TM_{02} mode because the patch length L_R is λ_d. Microstrip antennas operating at TM_{02} mode can produce dual symmetric radiation beams [19, 20], thus the upper band is operating with dual beams. By selecting the antenna dimensions properly, the three resonant frequencies f_L, f_M, and f_U are well excited, and a triple-band microstrip antenna can be achieved, which has a single beam across the lower and middle bands,

respectively, and dual beams across the upper band. The design guidance for the proposed antenna is as follows.

First Step: The design of the proposed antenna begins with the design of a conventional microstrip antenna operating at the upper band, and the initial dimensions of this conventional microstrip antenna can be calculated by formulas (1)–(5) given in [21].

$$W_R = \frac{c_0}{2f_r}\sqrt{\frac{2}{\varepsilon_r+1}} \tag{1}$$

$$\varepsilon_{eff} = \frac{\varepsilon_r+1}{2} + \frac{\varepsilon_r-1}{2}\left[1+\frac{12h}{W_R}\right]^{-\frac{1}{2}} \tag{2}$$

$$L_R = \frac{c_0}{2f_r\sqrt{\varepsilon_{eff}}} - 2\Delta L_R \tag{3}$$

$$\Delta L_R = 0.412h\frac{(\varepsilon_{eff}+0.3)\cdot(W_R/h+0.264)}{(\varepsilon_{eff}-0.258)\cdot(W_R/h+0.8)} \tag{4}$$

$$L_G = L_R + 6h,\ W_G = W_R + 6h \tag{5}$$

Considering that the upper band was conceived to operate in the range of 5 to 6 GHz, 5.5 GHz was selected as the initial value of f_r. Meanwhile, the thickness of the used air substrate $h = 3$ mm and its relative permittivity $\varepsilon_r = 1$ should be taken into consideration. Thereafter, the electromagnetic software HFSS was used to fine-tune the initial dimensions of this conventional microstrip antenna with the objective that its impedance matches well at 5.5 GHz.

Second Step: Extend the patch length to two times of that in the fine-tuned conventional microstrip antenna in the first step, and the patch width in the first step is kept unchanged. Thus a rectangular patch with its length L_R of λ_d is obtained, and its simulated reflection coefficient is shown in Fig. 3. A patch antenna with its length of λ_d can have a dual-beam radiation pattern [20]. Thus, a rectangular patch antenna operating with a dual-beam radiation pattern is achieved in this step.

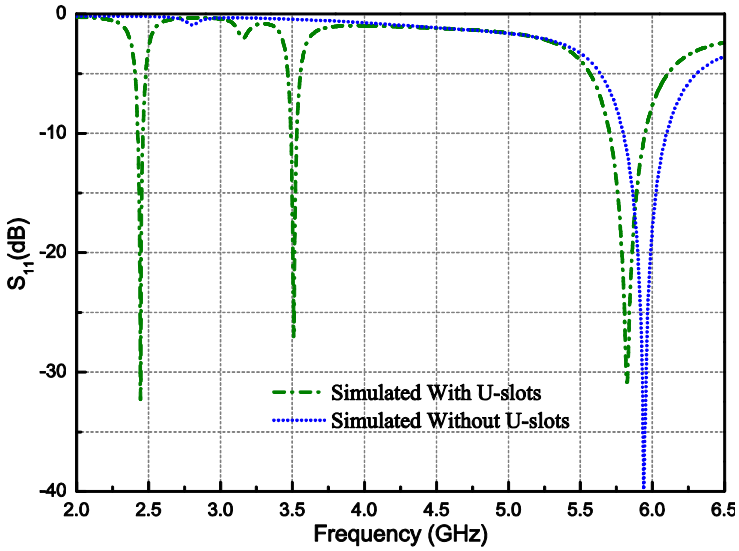

Figure 3. Simulated reflection coefficients of the proposed antenna without/with the U-slots.

Third Step: Two identical U-slots, which are used to create the lower and middle bands, were cut symmetrically on the surface of the rectangular patch with its length L_R of λ_d. For simplicity, the width U_C of the U-slot is fixed at 1 mm in the design process.

Fourth Step: By following the above three steps, the initial dimensions of the proposed antenna were achieved. Thereafter, an optimization process was carried out to determine the final dimensions

of the parameters including the feed position. The objective in this optimization was to ensure the impedance match well at the three resonant frequencies f_L, f_M, and f_U, and the simulated reflection coefficient of the proposed antenna with the U-slots is shown in Fig. 3.

From the above-mentioned design guidance, the proposed antenna's patch size (defined by both the patch length L_R and width W_R) is determined by the upper resonant frequency and not by the lower resonant frequency as most other multi-band antennas do. Specifically speaking, for the proposed antenna, the patch size was firstly achieved by the upper resonant frequency, that is to say, the patch length L_R is calculated by formula (3) at the upper resonant frequency and is λ_d instead of $\lambda_d/2$. The patch width W_R is calculated by formula (1) at the upper resonant frequency. Then create lower operating bands by cutting slots in the patch of the proposed antenna without increasing the antenna's overall area. For most other multi-band antennas, such as antennas in [8–10, 12–14], where their patch sizes were firstly achieved by the lower resonant frequency, create higher operating bands by cutting slots in the patch.

2.3. Parametric Study

Figure 4 shows the simulated reflection coefficients (S_{11}) for the proposed antenna with the variation of d_V. Observe that with the increase of d_V, the lower resonant frequency f_L of the lower band shifts moderately to lower frequency; the middle resonant frequency f_M of the middle band shifts moderately to higher frequency; and the upper resonant frequency f_U of the upper band shifts moderately to higher frequency.

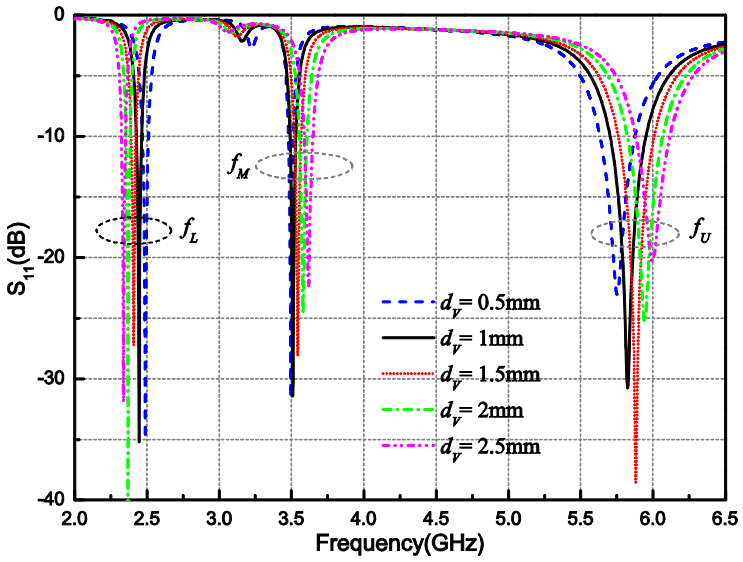

Figure 4. The simulated reflection coefficients (S_{11}) with the variation of d_V.

Figure 5 shows the simulated reflection coefficients for the proposed antenna with the variation of d_H. Observe that with the increase of d_H, the lower resonant frequency f_L shifts moderately to higher frequency; the middle resonant frequency f_M shifts considerably to higher frequency; and the upper resonant frequency f_U is almost kept unchanged.

Figure 6 shows the simulated reflection coefficients for the proposed antenna with the variation of arm length U_L. Observe that with the increase of U_L, the lower resonant frequency f_L shifts moderately to lower frequency; the middle resonant frequency f_M and the upper resonant frequency f_U both shift considerably to lower frequency; and f_M decreases faster than f_L and f_U. The reason for these phenomena is that the surface current on the patch has to flow around the U-slots. When U_L is increased, as observed from Figs. 2(a), (b), and (c), the surface current paths at all the three resonant frequencies are lengthened, and the resultant frequency decreases for f_L, f_M, and f_U. Indeed, the amplitude of the current distribution around the U-slots at f_M is stronger than that at f_L and f_U; therefore, the

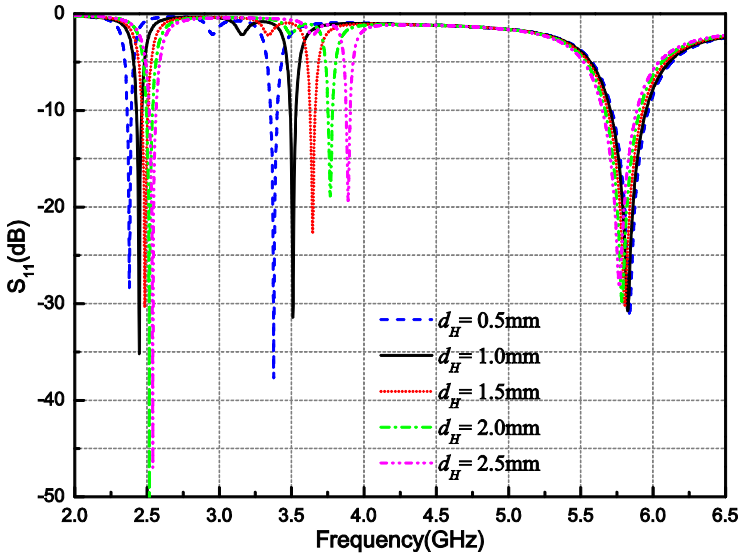

Figure 5. The simulated reflection coefficients (S_{11}) with the variation of d_H.

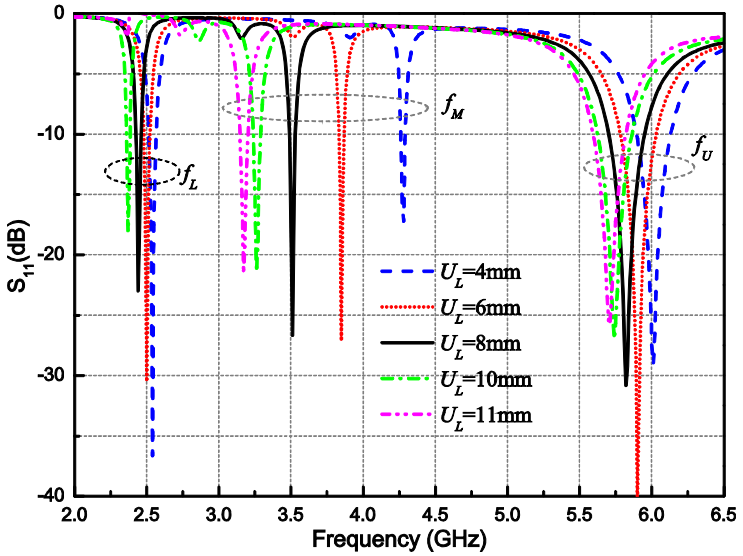

Figure 6. The simulated reflection coefficients (S_{11}) with the variation of U_L.

frequency decrease of f_M is faster than that of f_L and f_U. When U_L is greater than 10 mm, the proposed antenna exhibits a dual-band characteristic. In this case, the two operating frequencies are f_M and f_U. From the above-mentioned analysis, the three resonant frequencies can be adjusted by the tuning of U_L, which is more convenient than that reported in [18], where the two resonant frequencies can be adjusted through the shorting walls connected between the square ring patch and the ground plane. Indeed, also by tuning U_L, the proposed antenna can switch from a triple-band one to a dual-band one.

3. RESULTS AND DISCUSSIONS

The prototype of the proposed antenna is shown in Fig. 7, and observe that its structure is simple, simpler than many other antennas designed for realizing triple-band characteristic, such as antennas in [1–5] and [12–14]. The measured and simulated reflection coefficients S_{11} are shown in Fig. 8, and

Figure 7. Photograph of the proposed antenna.

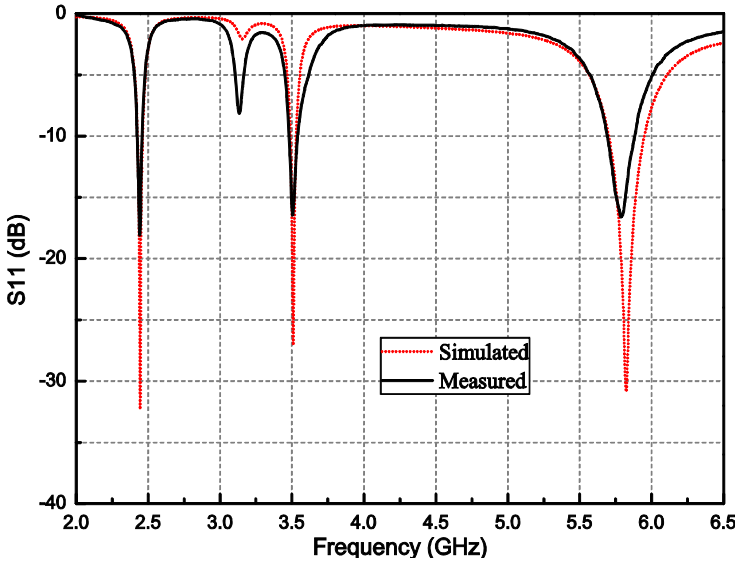

Figure 8. The measured and simulated reflection coefficients (S_{11}) of the proposed antenna.

they are in good agreement. The measured impedance bandwidths with $S_{11} \leq -10$ dB of the lower, middle, and upper operating bands are 1.39% (34 MHz) from 2.424 to 2.458 GHz, 1.71% (60 MHz) from 3.479 to 3.539 GHz, and 3.28% (190 MHz) from 5.692 to 5.882 GHz, respectively. Those simulated ones are 1.47% (36 MHz) from 2.426 to 2.462 GHz, 1.14% (40 MHz) from 3.489 to 3.529 GHz, and 4.24% (247 MHz) from 5.702 to 5.949 GHz), respectively. The measured three resonant frequencies are 2.442 GHz, 3.505 GHz, and 5.787 GHz, respectively, and those simulated ones are 2.444 GHz, 3.509 GHz, and 5.823 GHz, respectively. The three operating bands and resonant frequencies are frequently used in WLAN 2.4 GHz, 3.5 GHz of 5G (the fifth-generation mobile communication) operation, and WLAN 5.8 GHz [22]. The measured frequency ratios are: $f_U/f_L = 2.37$ and $f_M/f_L = 1.44$. Both the measured and simulated reflection coefficient S_{11} results demonstrate that the proposed antenna has a promising aspect that its impedance matches well at the three resonant frequencies with only one single feed point. The discrepancy between the measured and simulated reflection coefficients S_{11} is due to the fabrication tolerance and assemble errors. The bandwidths of the three operating bands can be further expanded by increasing the thickness of the air substrate and accompanied with aperture coupled feed or a cross-shaped probe feed; however, this introduces a complicated antenna structure.

The measured and simulated normalized radiation patterns at 2.442 GHz and 3.505 GHz are shown in Fig. 9 and Fig. 10, respectively. The simulated three-dimensional pattern at 5.787 GHz is shown in Fig. 11(a). The measured and simulated normalized radiation patterns at 5.737 GHz, 5.787 GHz, and 5.837 GHz in the yz-plane are shown in Figs. 11(b), (c), and (d), respectively. From Fig. 9, Fig. 10,

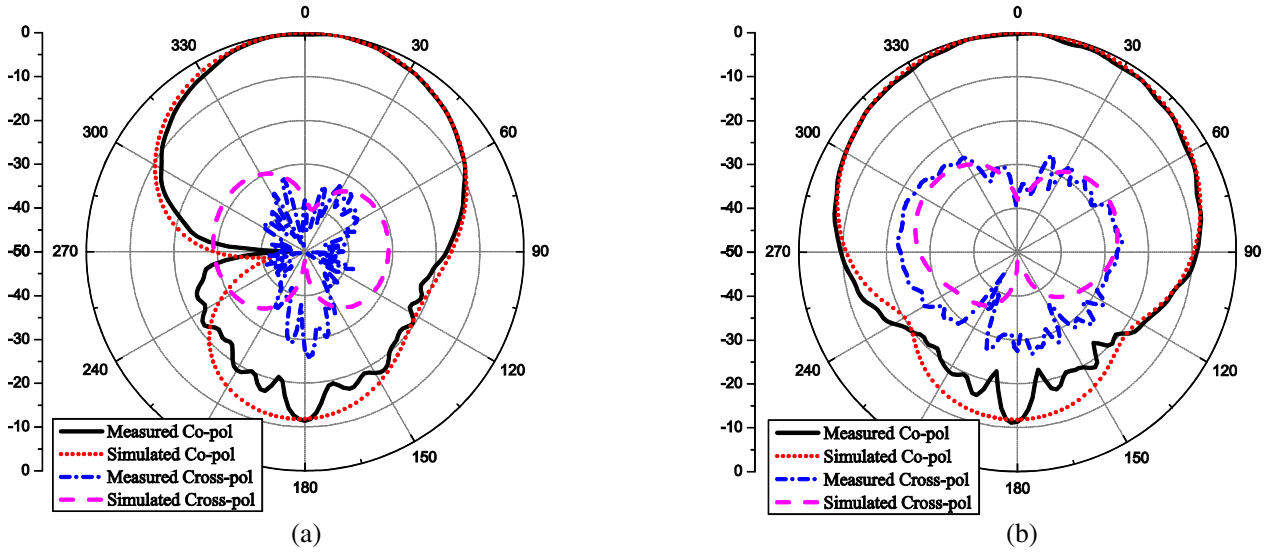

Figure 9. Measured and simulated normalized radiation patterns of the proposed triple-band antenna at 2.442 GHz: (a) yz plane; (b) xz plane.

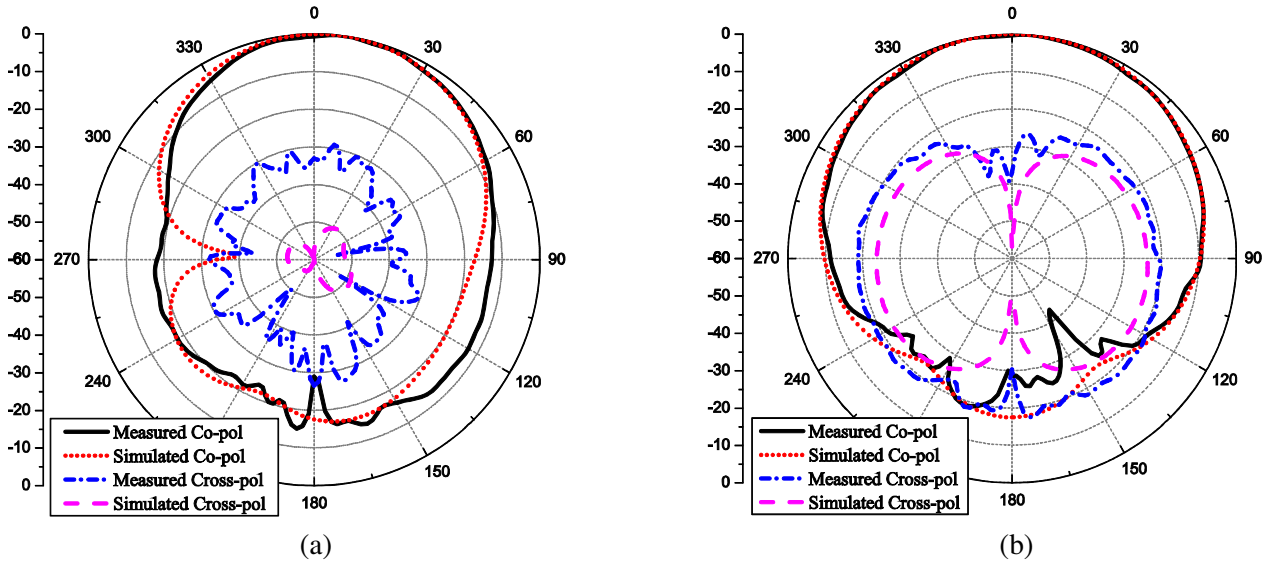

Figure 10. Measured and simulated normalized radiation patterns of the proposed triple-band antenna at 3.505 GHz: (a) yz plane; (b) xz plane.

and Figs. 11(b)–(d), observe that in all xz-planes and yz-planes, the measured and simulated results for the co-polarization patterns are in good agreement. Meanwhile, all the measured cross-polarization levels are satisfactorily low and below −18 dB for the worst case, which is benefited from the symmetric antenna geometry. Observe that the measured cross-polarization level is 15–20 dB higher than the simulated one in Fig. 10(a), Figs. 11(b), (c), and (d), respectively. Similar phenomenon has been reported in our previous study [23]. There are two reasons for this phenomenon. One is the limitation of the used anechoic chamber, i.e., the effective dynamic range of our anechoic chamber was lower than the simulated cross-polarization levels, thus the measured signals suffer from this limitation during the measurement. The other reason is the radiation from the induced currents caused by the RF cables and connectors feeding the antenna in a close proximity, which alters the radiation pattern during the measurement.

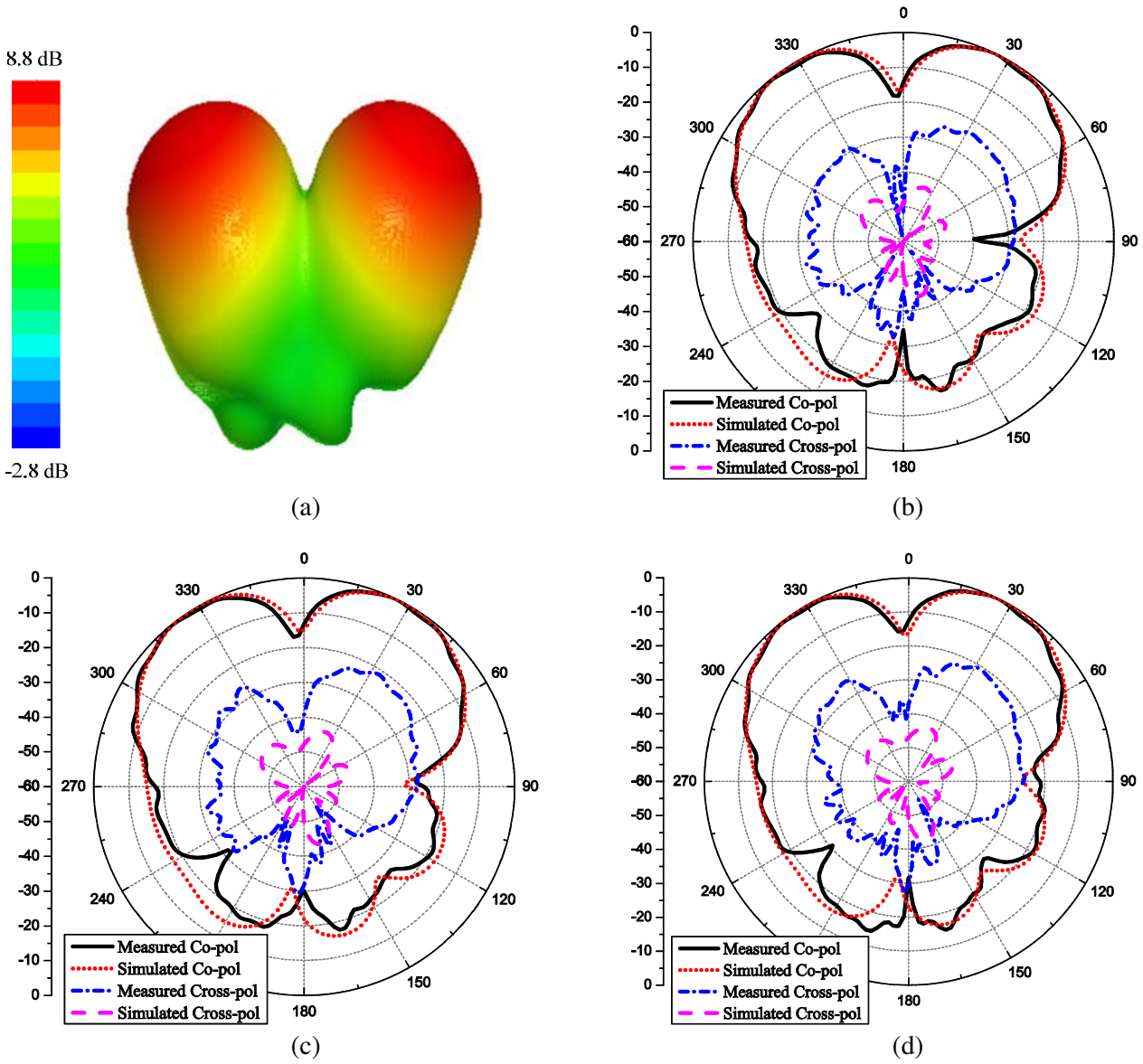

Figure 11. Measured and simulated normalized radiation patterns of the proposed triple-band antenna: (a) Simulated three-dimensional radiation pattern at 5.787 GHz; (b) 5.737 GHz (yz-plane); (c) 5.787 GHz (yz-plane); (d) 5.837 GHz (yz-plane).

From Fig. 9 and Fig. 10, observe that stable unidirectional single beam radiation pattern is achieved at the lower and middle bands, respectively. The measured and simulated gains in the broadside direction at 2.442 GHz are 6.2 dBi and 5.8 dBi, respectively, and those at 3.505 GHz are 5.5 dBi and 7.1 dBi, respectively. From Figs. 11(a)–(d), observe that dual-beam radiation pattern is achieved at the upper band, and the measured and simulated gains in the frequencies of the upper band are tabulated in Table 2. At 5.787 GHz, the measured gains of the left and right beams in the yz-plane are 8.2 dBi directed at $-38°$ and 8.4 dBi directed at 26°, respectively. Both the squints of the two beams are within 2° across the antenna operating band; meanwhile, the maximum difference between the maxima of the two beams is 0.3 dBi across the antenna operating band. The maximum difference between the beams' maxima is a crucial criterion to evaluate the performance of a multi-beam antenna.

A comparison on performances between the proposed antenna and the previous dual-band and triple-band patch antennas is shown in Table 3. Observe that the proposed antenna has the advantages of higher gain, dual-beam across one band, and a smaller radiating element volume simultaneously.

Table 2. The measured and simulated directions and gains for the left and right beams of the proposed antenna in the yz-plane at 5.737 GHz, 5.787 GHz, and 5.837 GHz.

Frequency (GHz)	Left Beam				Right Beam			
	Direction (θ_m°)		Gain (dBi)		Direction (θ_m°)		Gain (dBi)	
	S	M	S	M	S	M	S	M
5.737	-32	-40	8.9	8.1	29	26	8.8	8.5
5.787	-31	-38	8.8	8.2	29	26	8.8	8.4
5.837	-31	-38	8.7	7.9	28	26	8.6	8.4
Simulated, S; measured, M.								

Table 3. Comparison with previous works.

Reference		[9]	[10]	[12]	[13]	**This work**
Number of operating bands		2	2	3	3	3
Resonant frequencies(GHz) & Bandwidth(%)	**The lower band**	1.701GHz 0.2%	1.547GHz, 1.26%	0.84GHz, 0.7%	0.926GHz, 2.2%	2.442GHz, 1.39%
	The middle band	8.088GHz 3.1%	1.87GHz, 1.74%	1.8GHz, 1.5%	1.57GHz, 5.8%	3.505GHz, 1.71%
	The upper band	–	–	2.45GHz, 0.7%	2.47GHz, 2.8%	5.787GHz, 3.28%
Gain(dBi)	**The lower resonant frequency**	NG	1.2 dBi	3.1 dBi	0.32 dBi	6.2 dBi
	The middle resonant frequency	NG	3.0 dBi	4.4 dBi	1.2 dBi	5.5 dBi
	The upper resonant frequency	–	–	2 dBi	1.5 dBi	**8.2 dBi/8.4 dBi**
Radiation Beam	**The lower band**	Single beam	Single beam	Single beam	Single beam	Single beam
	The middle band	Single beam	Single beam	Single beam	Single beam	Single beam
	The upper band	–	–	Single beam	Single beam	**Dual-beam**
Radiating element volume related to the lower frequency(λ_g is the wavelength in the substrate)		$0.56\lambda_g \times 0.48\lambda_g \times 0.02\lambda_g$	$0.43\lambda_g \times 0.32\lambda_g \times 0.02\lambda_g$	$0.42\lambda_g \times 0.42\lambda_g \times 0.01\lambda_g$	$0.13\lambda_g \times 0.14\lambda_g \times 0.01\lambda_g$	$0.37\lambda_g \times 0.16\lambda_g \times 0.02\lambda_g$
Radiating element volume related to the upper frequency(λ_g is the wavelength in the substrate)		–	–	$1.21\lambda_g \times 1.21\lambda_g \times 0.04\lambda_g$	$0.35\lambda_g \times 0.36\lambda_g \times 0.03\lambda_g$	$0.87\lambda_g \times 0.39\lambda_g \times 0.06\lambda_g$

4. CONCLUSION

A novel triple-band microstrip antenna with two U-slots is presented and investigated. The antenna's structure is simple. Unidirectional single radiation beam is achieved at each of the lower and middle bands, and dual radiation beams are achieved at the upper band. The measured gains at 2.442 GHz and 3.505 GHz in the broadside directions are 6.2 dBi and 5.5 dBi, respectively. The measured gains for the dual beams at 5.787 GHz in the yz-plane are 8.2 dBi directed at -38° and 8.4 dBi directed at 26°. The proposed antenna has a smaller radiating element volume and a higher gain than the antennas in [9, 10, 12]. The proposed antenna can be a candidate for multi-frequency wireless communication system of WLAN 2.4 GHz, 3.5 GHz in 5G operation, and WLAN 5.8 GHz.

ACKNOWLEDGMENT

This work was supported by the National Natural Science Foundation of China under Grant 61701041 and Grant 61401042, and by Beijing Key Laboratory of Work Safety Intelligent Monitoring (Beijing University of Posts and Telecommunications).

REFERENCES

1. Wen, R., "Compact planar triple-band monopole antennas based on a single-loop resonator," *Electronics Letters*, Vol. 49, 916–918, 2013.
2. Kang, L., H. Wang, X. H. Wang, and X. Shi, "Compact ACS-fed monopole antenna with rectangular SRRS for tri-band operation," *Electronics Letters*, Vol. 50, 1112–1114, 2014.
3. Chouti, L., I. Messaoudene, T. A. Denidni, and A. Benghalia, "Triple-band CPW-fed monopole antenna for WLAN/WiMAX applications," *Progress In Electromagnetics Research Letters*, Vol. 69, 1–7, 2017.
4. Chen, S. W., D. Y. Wang, and W. H. Tu, "Dual-band/tri-band/broadband CPW-fed stepped-impedance slot dipole antennas," *IEEE Transactions on Antennas and Propagation*, Vol. 62, 485–490, 2014.
5. Dang, L., Z. Y. Lei, Y. J. Xie, G. L. Ning, and J. Fan, "A compact microstrip slot triple-band antenna for WLAN/WiMAX applications," *IEEE Antennas and Wireless Propagation Letters*, Vol. 9, 1178–1181, 2010.
6. Zhang, T., W. Hong, and K. Wu, "A low-profile triple-band triple-polarization antenna with two triangular rings," *IEEE Antennas and Wireless Propagation Letters*, Vol. 14, 378–381, 2015.
7. Katyal, A. and A. Basu, "Compact and broadband stacked microstrip patch antenna for target scanning applications," *IEEE Antennas and Wireless Propagation Letters*, Vol. 16, 381–384, 2017.
8. Rahman, M. A., E. Nishiyama, and I. Toyoda, "A dual-band slot-embedded microstrip antenna for dual-polarization operation," *Progress In Electromagnetics Research M*, Vol. 63, 141–149, 2018.
9. Esfahlani, S. H. S., A. Tavakoli, and P. Dehkhoda, "A compact single-layer dual-band microstrip antenna for satellite applications," *IEEE Antennas and Wireless Propagation Letters*, Vol. 10, 931–934, 2011.
10. Chen, H., "Single-feed dual-frequency rectangular microstrip antenna with a π-shaped slot," *IEE Proceedings — Microwaves, Antennas and Propagation*, Vol. 148, 60–64, 2001.
11. Fortaki, T., L. Djouane, F. Chebara, and A. Benghalia, "On the dual-frequency behavior of stacked microstrip patches," *IEEE Antennas and Wireless Propagation Letters*, Vol. 7, 310–313, 2008.
12. Chen, W., Y. Li, H. Jiang, and Y. Long, "Design of novel tri-frequency microstrip patch antenna with arc slots," *Electronics Letters*, Vol. 48, 609–611, 2012.
13. Patel, R. H., A. Desai, and T. K. Upadhyaya, "An electrically small antenna using defected ground structure for RFID, GPS and IEEE 802.11 a/B/G/S applications," *Progress In Electromagnetics Research Letters*, Vol. 75, 75–81, 2018.
14. Bao, X. L. and M. J. Ammann, "Compact concentric annular-ring patch antenna for triple-frequency operation," *Electronics Letters*, Vol. 42, 1129–1130, 2006.
15. Kuo-Hui, L., M. A. Ingram, and E. O. Rausch, "Multibeam antennas for indoor wireless communications," *IEEE Transactions on Communications*, Vol. 50, 192–194, 2002.
16. Lu, H., F. Liu, Y. Liu, and S. Huang, "Single-layer single-patch wideband dual-beam E-shaped patch antenna," *2017 IEEE 5th International Symposium on Electromagnetic Compatibility*, 1–3, (EMC-Beijing), 2017.
17. Chen, C., Y. Guo, and H. Wang, "Wideband symmetrical cross-shaped probe dual-beam microstrip patch antenna," *IEEE Antennas and Wireless Propagation Letters*, Vol. 14, 622–625, 2015.
18. Chen, S.-H., J.-S. Row, and C.-Y.-D. Sim, "Single-feed square-ring patch antenna with dual-frequency operation," *Microwave and Optical Technology Letters*, Vol. 49, 991–994, 2007.

19. Carver, K. and J. Mink, "Microstrip antenna technology," *IEEE Transactions on Antennas and Propagation*, Vol. 29, 2–24, 1981.
20. Lo, Y., D. Solomon, and W. Richards, "Theory and experiment on microstrip antennas," *IEEE Transactions on Antennas and Propagation*, Vol. 27, 137–145, 1979.
21. Liu, S., W. Wu, and D. G. Fang, "Single-feed dual-layer dual-band E-shaped and U-slot patch antenna for wireless communication application," *IEEE Antennas and Wireless Propagation Letters*, Vol. 15, 468–471, 2016.
22. Kuhestani, H., M. Rahimi, Z. Mansouri, F. B. Zarrabi, and R. Ahmadian, "Design of compact patch antenna based on metamaterial for WiMAX applications with circular polarization," *Microwave and Optical Technology Letters*, Vol. 57, 357–360, 2015.
23. Lu, H. X., F. Liu, M. Su, and Y. A. Liu, "Design and analysis of wideband U-slot patch antenna with U-shaped parasitic elements," *International Journal of RF and Microwave Computer-Aided Engineering*, Vol. 28, e21202, 2018.